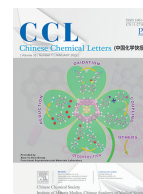




ELSEVIER

Contents lists available at ScienceDirect

Chinese Chemical Letters

journal homepage: [www.elsevier.com/locate/ccllet](http://www.elsevier.com/locate/ccllet)

# Carbon dots embedded nanofiber films: Large-scale fabrication and enhanced mechanical properties

Chang Liu<sup>1</sup>, Rui Cheng<sup>1</sup>, Jiazhuang Guo, Ge Li, He Li, Hong-Gang Ye, Zhi-Bin Liang, Cai-Feng Wang\*, Su Chen\*

State Key Laboratory of Materials-Oriented Chemical Engineering, College of Chemical Engineering, and Jiangsu Key Laboratory of Fine Chemicals and Functional Polymer Materials, Nanjing Tech University, Nanjing 210009, China

## ARTICLE INFO

### Article history:

Received 6 May 2021

Revised 23 June 2021

Accepted 28 June 2021

Available online 7 July 2021

### Keywords:

Carbon dots

Mass production

Solution blow spinning

Nanofiber

Mechanical properties

## ABSTRACT

Valuable application prospects and large-scale production technologies are powerful driving forces for the development of materials science. Carbon dots (CDs) are a kind of promising carbon-based fluorescent nanomaterials, which possess wide application prospects based and even beyond the fluorescence properties. Herein, we report the fast and high-yield synthesis of CDs and the large-scale preparation of fluorescent nanofiber films with enhanced mechanical properties. CDs were prepared from magnetic hyperthermia treatment of citric acid and carbamide, with the output of 25.37 g in a single batch. The as-prepared CDs exhibit a high absolute photoluminescence (PL) quantum yield (QY) of 67% and wonderful dispersibility in polar solvents. Then, solution blow spinning of CDs and polymer matrixes of alcohol soluble polyurethane (APU) and polyacrylonitrile (PAN) led to large-area fluorescent CDs-embedded nanofiber films, APU/CDs (size: 120 cm × 18 cm) and PAN/CDs (size: 120 cm × 22 cm), respectively. The resultant large-area APU/CDs and PAN/CDs nanofiber films have dramatically enhanced mechanical properties, to show integrated improvement of tensile strength and elongation.

© 2021 Published by Elsevier B.V. on behalf of Chinese Chemical Society and Institute of Materia Medica, Chinese Academy of Medical Sciences.

Carbon-based nanomaterials are a kind of environmentally friendly, accessible and promising star materials [1–3]. As a burgeoning member of carbon-based nanomaterials, carbon dots (CDs) have aroused increasing interests owing to their superb biocompatibility, low toxicity and good photoluminescence (PL) [4]. Taking advantage of their tunable fluorescence, CDs could find applications in biological imaging [5], sensors [6], anti-counterfeiting [7], luminescent solar concentrators [8], and LED devices [9]. Besides, CDs have diverse surface functional groups, which make CDs useful for broader applications beyond their PL properties [10], such as surfactant [11], reducing reagent [12], induce crystallization [13], consolidant [14], antirust [15], antifreeze [16], lubricant [17], reinforcing reagent [18,19].

Particularly, enhancing mechanical properties of polymer materials by CDs is a project worth in-depth research, since strong polymer materials are widely used in every aspect of human life. In this respect, Guo's group used CDs as high-functionality cross-linkers to fabricate strong yet tough *cis*-1,4-polyisoprene elastomer

[20]. Hu *et al.* prepared polymer-carbon dot-ferric ion nanocomposite hydrogels [21]. Wu's group applied N-doped CDs as dual role of crosslinking and reinforcing reagents to improve mechanical properties of chloroprene rubber [22]. Yu *et al.* [23] developed an *in-suit* compatibilizing method to prepare styrene-butadiene rubber/CDs composite with enhanced mechanical properties and good antioxidative ability. On the other hand, artificial polymeric fibers such as polyacrylonitrile (PAN) and polyurethane (PU) fibers are very useful in various applications [24]. For instance, PAN fibers are regarded as the best precursors of carbon fibers, indicating the potential application in high-strength materials [25]. The large-scale fabrication of artificial polymeric fibers with high performance like good optical/mechanical properties is highly desirable yet challenging. In this context, some spinning techniques have been developed for fabrication of various artificial polymeric fibers [26]. In particular, solution blow spinning could spin diverse polymers with use of high-speed blowing air as driving force [27], and we expected that this spinning technique could be exploited as easy-to-perform platform to realize the fast and mass production of size-tunable functional polymer fibers.

To this end, we demonstrate the mass production of CDs for use in large-scale preparation of nanofiber films with good fluorescence and enhanced mechanical properties. We employed a

\* Corresponding authors.

E-mail addresses: caifengwang@njtech.edu.cn (C.-F. Wang), chensu@njtech.edu.cn (S. Chen).

<sup>1</sup> Both the authors contributed equally to this work.

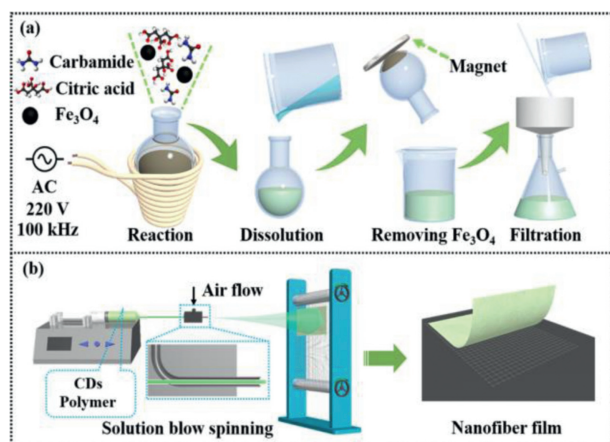


**Fig. 1.** (a) Schematic operating procedure for synthesizing CDs by magnetic hyperthermia method. (b) Schematic fabrication of large-scale CDs-embedded nanofiber films by solution blow spinning.

magnetic hyperthermia method [28,29] to synthesize CDs in large scale by solid-solid reaction from citric acid and carbamide, guaranteeing the mass use of CDs for further large-scale application. Fig. 1a displays the main operating steps of the fabrication process for CDs, including reaction, dissolution, removing Fe<sub>3</sub>O<sub>4</sub> and filtration. The CDs powder was collected after the process of concentration and freeze drying. In a single batch, the output of CDs was 25.37 g. Moreover, the resultant CDs have a good dispersibility in polar solvents, and exhibit blue-green PL with PL QY of 67% and mono-exponential PL decay dynamics. Subsequently, we fabricated large-area CDs-embedded polymeric nanofiber films with good fluorescence and enhanced mechanical properties *via* solution blow spinning (Fig. 1b).

Alcohol soluble polyurethane (APU) and polyacrylonitrile (PAN) were chosen as polymer matrix, to afford APU/CDs and PAN/CDs nanofibers with mean diameters of 700 nm and 560 nm, respectively. Large-area nanofiber films of APU/CDs (120 cm × 18 cm) and PAN/CDs (120 cm × 22 cm) were fabricated, to exhibit uniform fluorescence and enhanced mechanical properties. Specifically, upon the incorporation of 10 wt% CDs, the tensile strength and elongation of the APU/CDs nanofiber film are 2.9 and 1.9 times that of the pure APU nanofiber film, and the PAN/CDs nanofiber film is 2.58 and 2.0 times the tensile strength and elongation of the pure one, respectively. This work paves a way for mass production of CDs toward their use in large-scale preparation of nanofiber films with good optical properties and enhanced mechanical performance.

CDs were synthesized in large scale by solid-solid reaction from citric acid and carbamide *via* a magnetic hyperthermia method. The magnetic hyperthermia method can realize rapid heating in a high-efficiency way, which has been applied in metallurgical industry [30]. In our previous works, we have developed magnetic hyperthermia method for the synthesis of semiconductor nanocrystals [31] and CDs [28,29]. During a representative large-scale synthesis process of CDs by magnetic hyperthermia method, the control unit in magnetic hyperthermia reactor supplied a 100 kHz alternating current to drive the induction coil. Fe<sub>3</sub>O<sub>4</sub> nanoparticles were served as the heating source in the induced magnetic field to heat the precursors, wherein the temperature could reach 250 °C in 5 s. The entire reaction process was sustained about 90 s. The post-processing includes dissolution, removal of Fe<sub>3</sub>O<sub>4</sub>, filtration, concentration and freeze drying. In a single batch of reaction, the output of CDs was 25.37 g (Fig. 2a). The large-scale production of CDs guarantees their mass use in further large-scale application.

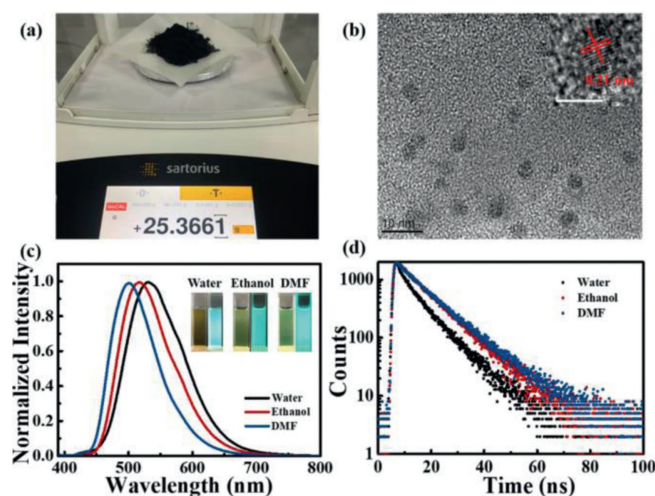


**Fig. 2.** (a) Photograph of CDs prepared in a single batch of reaction. (b) TEM image of CDs. Inset: HRTEM image of the CDs (scale bar: 5 nm). (c) PL spectra of CDs dispersed in water, ethanol and DMF. Inset pictures: photographs of CDs solutions taken under daylight and 365 nm UV light. (d) Time-resolved PL decay curves of CDs dispersed in water, ethanol and DMF.

The morphology of CDs was confirmed by TEM measurement. As shown in Fig. 2b, the CDs has a uniform dispersibility without aggregation. The average size of CDs is 3.4 nm (Fig. S1 in Supporting information). The high-resolution TEM (HRTEM) image shows that the CDs have obvious lattice fringes with a spacing of 0.21 nm, which could be attributed to the (100) plane of graphitic carbon [32,33]. The XRD pattern of the CDs shown in Fig. S2a (Supporting information) displays a broad peak centered around 25°, which is attributed to highly disordered carbon atoms [34]. FT-IR analysis was also performed (Fig. S2b in Supporting information), which indicates that there are abundant polar functional groups on the surface of CDs, such as N–H (3444 cm<sup>-1</sup>), O–H (3434 cm<sup>-1</sup>), C=O (1647 cm<sup>-1</sup>) and C–O (1131 cm<sup>-1</sup>) [35,36]. These polar functional groups ensure CDs have a good dispersibility in polar solvents. The XPS analysis further confirms the existence of the polar functional groups. Fig. S3a (Supporting information) displays three typical peaks of O (532 eV), N (400 eV) and C (285 eV). The high-resolution XPS results are shown in Figs. S3b–d (Supporting information). The C 1s bands are deconvoluted into four peaks at 288.6 eV, 287.9 eV, 286.4 eV and 284.8 eV, respectively, corresponding to C–O–C/C=O, C=O, C–OH and C=C, respectively [37–40]. The N 1s bands contain two peaks at 399.7 eV and 401.3 eV for pyrrolic N and graphene N [41,42]. The O 1s bands analysis reveals the presence of C–O (532.7 eV) and C=O (531.4 eV) [43,44].

Thanks to the abundant polar functional groups on the surface, the CDs have good dispersibility in polar solvents such as water, ethanol and DMF, while their solubility in nonpolar solvents like toluene or hexane is poor. Fig. 2c displays PL spectra of CDs dispersed in different polar solvents. The inset pictures display the CDs solutions taken under daylight and 365 nm UV light. Under excitation at 400 nm, the maximum emissions gradually shift from 500 nm to 531 nm, the full width at half maximums (FWHM) cover 82–104 nm. Moreover, the PL QYs of CDs dispersed in water, ethanol and DMF are 41%, 67% and 58% respectively. The results reveal the truth that the PL properties of CDs prepared by magnetic hyperthermia method are comparable to those of CDs prepared by other methods such as hydrothermal, pyrolysis and microwave methods [45–47]. The time-resolved PL decay curves of CDs dispersed in different polar solvents were measured, which are shown in Fig. 2d. PL decay dynamics of CDs dispersed in water, ethanol and DMF all close to mono-exponential, and the PL life-

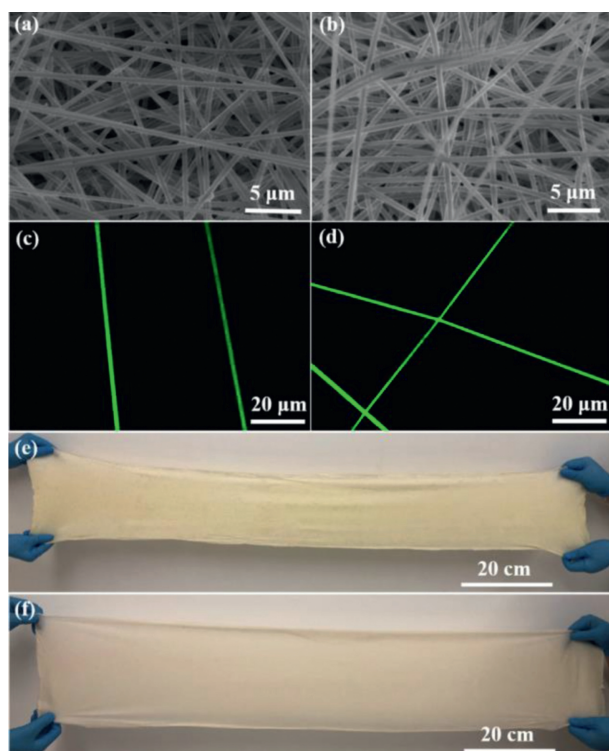


**Fig. 3.** SEM images of APU/CDS (a) and PAN/CDS (b) nanofiber films. PL images of APU/CDS (c) and PAN/CDS (d) nanofibers taken by laser scanning confocal microscope under a 405 nm excitation light. The photographs of APU/CDS (e) and PAN/CDS (f) nanofiber films.

times are 7.9, 10.0 and 10.8 ns respectively. The further research of PL properties is shown in Figs. S4a–c (Supporting information). The CDs dispersed in different polar solvents all reveal characteristic excitation-dependent PL property, which is common in fluorescent CDs [48,49]. This behavior should be attributed to the surface state affecting the band gap of CDs [50]. Fig. S4d shows the UV–vis absorption spectra of CDs dispersed in different polar solvents. The CDs dispersed in water exhibit a strong adsorption band at 340 nm, which might be assigned to the trapping of excited-state energy by surface state [51]. Moreover, CDs dispersed in different solvents all exhibit an adsorption band at about 415 nm, which might be originated from  $n-\pi^*$  transition of C=O bonds.

We realized the fabrication of large-area CDs-embedded polymeric nanofiber films with good fluorescence and enhanced mechanical properties *via* solution blow spinning. Thanks to the good dispersibility of CDs in polar solvents, we fabricated APU/CDS and PAN/CDS nanofiber films with different concentrations of CDs. For convenience, we abbreviated 10 wt% of CDs in APU as APU/CDS-10%, and so on in a similar fashion. The specific experimental details are shown in Supporting information. The morphologies of APU/CDS (Fig. 3a) and PAN/CDS (Fig. 3b) nanofiber films were confirmed by SEM characterization. The solution blow spinning strategy afforded nanofibers of APU/CDS and PAN/CDS uniformly distributed over all the nylon mesh. Moreover, the mean diameters of nanofibers are 700 nm (APU/CDS) and 560 nm (PAN/CDS), which are comparable to those reported previously [52,53]. Furthermore, the CDs-embedded nanofibers still keep outstanding PL properties, overcoming the self-quenching of CDs usually occurring in solid state [54]. The PL images of nanofibers were recorded by laser scanning confocal microscope under a 405 nm excitation light (Figs. 3c and d). It is clear that the nanofibers exhibited uniform and bright fluorescence, which is the powerful evidence to prove that the CDs are dispersed uniformly in nanofibers and

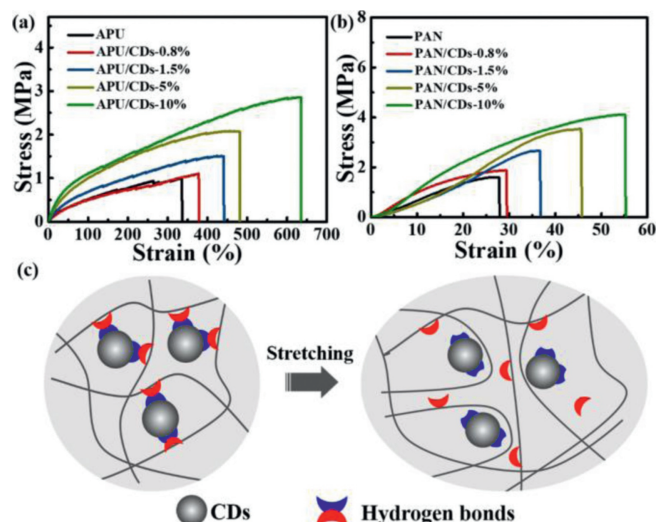


**Fig. 4.** Strain-stress curves of APU/CDS (a) and PAN/CDS (b) nanofiber films. (c) The schematic of mechanism for the increased mechanical properties.

no self-quenched phenomenon. The PL properties of APU/CDS and PAN/CDS nanofiber films are shown in Fig. S5 (Supporting information). It can be seen that the PL peaks are centered at 500 nm and 480 nm, and the lifetimes are 10.8 ns and 11.6 ns, respectively. Besides, we investigated the influence of CDs on the transparency and wettability of the nanofiber films. The incorporation of CDs into the PAN/CDS nanofiber films does not change much the films transparency. Whereas, the nanofiber films become more hydrophilic with the increase of the concentration of CDs (Fig. S6 in Supporting information), which may be due to the abundant polar functional groups on the surface of CDs. With the assistance of solution blow spinning machine, large-area nanofiber films of APU/CDS and PAN/CDS were fabricated (Figs. 3e and f), with size of 120 cm × 18 cm and 120 cm × 22 cm, respectively.

Benefiting from the abundant functional groups on the surface of CDs, CDs are easy to show interaction with polymer matrix, for example, hydrogen bonds [55]. Based on this, we investigated the mechanical properties of APU/CDS and PAN/CDS nanofiber films with different concentrations of CDs. Stress-strain curves of APU/CDS and PAN/CDS nanofiber films are shown in Figs. 4a and b. Limited by the solubility of CDs in ethanol and DMF, the highest concentration of CDs was fixed at 10 wt% for both APU and PAN systems. If further adding CDs at the highest concentration, the visible solid particles by naked eye would appear in the mixture, resulting in the ununiform distribution of CDs in the polymeric nanofibers. Significantly, the resultant large-area CDs-embedded polymeric nanofiber films have enhanced mechanical properties. For APU/CDS nanofiber films, the tensile strength increases from 0.98 MPa to 2.86 MPa, while the elongation rises from 335% to 635% with the increasing concentration of CDs. The stress-strain curves of PAN/CDS nanofiber films exhibit the similar results. As shown in Fig. 4b, the tensile strength increases from 1.59 MPa to 4.11 MPa, while the elongation rises from 27% to 55% with the increasing concentration of CDs. The improved mechanical properties might be attributed to hydrogen bonds between CDs and polymer matrix, as shown in Fig. 4c. FT-IR and XPS characterizations confirmed that the surface of CDs exists abundant amino, carboxyl and hydroxide groups (Figs. S2b and S3), which are easy to form hydrogen bonds with APU and PAN polymer matrixes [56]. These hydrogen bonds serve as sacrificial units, which preferentially rupture to significantly consume energy under stretching [20]. On the other hand, a mass of knots form with the CDs as center, and these

knots also take on sectional mechanical stress during the stretching process [57].

In summary, we demonstrate the mass production of CDs for large-scale preparation of nanofiber films with good fluorescence and enhanced mechanical properties. CDs were synthesized by magnetic hyperthermia with the output of 25.37 g in a single batch. The as-prepared CDs exhibit a high absolute PL QY of 67% and wonderful dispersibility in polar solvents. Moreover, large-area fluorescent CDs-embedded nanofiber films were fabricated by solution blow spinning with CDs and polymer matrixes of APU and PAN, with sizes of 120 cm × 18 cm and 120 cm × 22 cm for APU/CDs and PAN/CDs nanofiber films, respectively. The resultant large-area APU/CDs and PAN/CDs nanofiber films have dramatically enhanced mechanical properties, to show integrated improvement of tensile strength and elongation. Specifically, the incorporation of 10 wt% CDs could double both the tensile strength and elongation of the nanofiber films. This work may bring a new insight into the application of CDs in polymer industry.

### Declaration of competing interest

The authors declare that they have no known competing financial interests or personal relationships that could have appeared to influence the work reported in this paper.

### Acknowledgments

This work was supported by the National Natural Science Foundation of China (Nos. 21736006 and 21978132), the National Key Research and Development Program of China (Nos. 2016YFB0401700 and 2018YFC1602800), the Fund of the State Key Laboratory of Materials-Oriented Chemical Engineering (Nos. ZK201704 and ZK201716), and the Priority Academic Program Development of Jiangsu Higher Education Institutions (PAPD).

### Supplementary materials

Supplementary material associated with this article can be found, in the online version, at doi:10.1016/j.ccl.2021.06.073.

### References

- [1] Y.P. Sun, B. Zhou, Y. Lin, et al., *J. Am. Chem. Soc.* 128 (2006) 7756–7757.
- [2] Y.Z. Lin, J.Y. Wang, Z.G. Zhang, et al., *Adv. Mater.* 27 (2015) 1170–1174.
- [3] L. Ai, Y.S. Yang, B.Y. Wang, et al., *Sci. Bull.* 66 (2021) 839–856.
- [4] X. Guo, C.F. Wang, Z.Y. Yu, L. Chen, S. Chen, *Chem. Commun.* 48 (2012) 2692–2694.
- [5] S.Y. Lu, L.Z. Sui, J.J. Liu, et al., *Adv. Mater.* 29 (2017) 1603443.
- [6] W.D. Li, Y. Liu, B.Y. Wang, et al., *Chin. Chem. Lett.* 30 (2019) 2323–2327.
- [7] J.Z. Guo, H. Li, L.T. Ling, et al., *ACS Sustain. Chem. Eng.* 8 (2020) 1566–1572.
- [8] Y.F. Zhou, D. Benetti, X. Tong, et al., *Nano Energy* 44 (2018) 378–387.
- [9] B.Y. Wang, Jian. Li, Z.Y. Tang, et al., *Sci. Bull.* 64 (2019) 1285–1292.
- [10] X.K. Xu, Y.D. Li, G.Q. Hu, et al., *J. Mater. Chem. C* 8 (2020) 16282–16294.
- [11] J.M. Zhu, X.H. Li, Y.Y. Zhang, et al., *Adv. Funct. Mater.* 28 (2018) 1803872.
- [12] M.J. Jing, J.F. Wang, H.S. Hou, et al., *J. Mater. Chem. A* 3 (2015) 16824–16830.
- [13] Q. Gao, J.M. Han, Z.F. Ma, *Biosens. Bioelectron.* 49 (2013) 323–328.
- [14] C. Zhu, Y.J. Fu, C.A. Liu, et al., *Adv. Mater.* 29 (2017) 1701399.
- [15] M.J. Cui, S.M. Ren, Q.J. Xue, et al., *J. Alloys Compd.* 726 (2017) 680–692.
- [16] G.Y. Bai, Z.P. Song, H.Y. Geng, et al., *Adv. Mater.* 29 (2017) 1606843.
- [17] H. Huang, H.L. Hu, S. Qiao, et al., *Nanoscale* 7 (2015) 11321–11327.
- [18] M. Hu, Y. Yang, X.Y. Gu, et al., *Macromol. Mater. Eng.* 300 (2015) 1043–1048.
- [19] P.R. Sreenath, S. Singh, M.S. Satyanarayana, P. Das, K.D. Kumar, *Polymer* 112 (2017) 189–200.
- [20] S.W. Wu, M. Qiu, Z.H. Tang, J. Liu, B.C. Guo, *Macromolecules* 50 (2017) 3244–3253.
- [21] Y. Hu, Y.Z. Li, D. Wang, et al., *Eur. Polym. J.* 95 (2017) 482–490.
- [22] L.M. Kong, Y. Zhu, G.S. Huang, J.R. Wu, *Compos. Commun.* 22 (2020) 100441.
- [23] P. Yu, G.Z. Jin, W.C. Wang, et al., *Compos. Commun.* 22 (2020) 100429.
- [24] T. Lin, H.X. Wang, X.G. Wang, *Adv. Mater.* 17 (2005) 2699–2703.
- [25] M.A. Al Faruque, R. Remadevi, J.M. Razal, M. Naebe, *J. Appl. Polym. Sci.* 137 (2020) 49264.
- [26] X.Y. Du, Q. Li, G. Wu, S. Chen, *Adv. Mater.* 31 (2019) 1903733.
- [27] T.T. Cui, J.F. Yu, Q. Li, et al., *Adv. Mater.* 32 (2020) 2000982.
- [28] Z.J. Zhu, R. Cheng, L.T. Ling, Q. Li, S. Chen, *Angew. Chem. Int. Ed.* 59 (2020) 3099–3105.
- [29] L.T. Ling, Z.J. Zhu, H.X. Shen, et al., *Ind. Eng. Chem. Res.* 59 (2020) 4968–4976.
- [30] M. Ognjanović, D.M. Stanković, Y. Ming, et al., *J. Alloy. Compd.* 777 (2019) 454–462.
- [31] L.T. Ling, W. Wang, C.F. Wang, S. Chen, *AIChE J.* 62 (2016) 2614–2621.
- [32] M.L. Liu, L. Yang, R.S. Li, et al., *Green Chem.* 19 (2017) 3611–3617.
- [33] Q. Chang, X.J. Han, C.R. Xue, J.L. Yang, S.L. Hu, *Chem. Commun.* 53 (2017) 2343–2346.
- [34] S.J. Zhu, Q.N. Meng, L. Wang, et al., *Angew. Chem. Int. Ed.* 125 (2013) 4045–4049.
- [35] H. Ding, J.S. Wei, P. Zhang, et al., *Small* 14 (2018) 1800612.
- [36] S.Y. Tao, S.Y. Lu, Y.J. Geng, et al., *Angew. Chem. Int. Ed.* 57 (2018) 2393–2398.
- [37] X. Miao, D. Qu, D.X. Yang, et al., *Adv. Mater.* 30 (2017) 1704740.
- [38] J. Briscoe, A. Marinovic, M. Sevilla, S. Dunn, M. Titirici, *Angew. Chem. Int. Ed.* 54 (2015) 4463–4468.
- [39] J.H. Shin, J. Guo, T.T. Zhao, Z.X. Guo, *Small* 15 (2019) 1900296.
- [40] J. Wang, C.F. Wang, S. Chen, *Angew. Chem. Int. Ed.* 124 (2012) 9431–9435.
- [41] S.Y. Lu, L.Z. Sui, M. Wu, et al., *Adv. Sci.* 6 (2019) 1801192.
- [42] H.F. Liu, Y.Q. Sun, Z.H. Li, et al., *Nanoscale* 11 (2019) 8458–8463.
- [43] C. Wang, T.T. Hu, Y.Y. Chen, Y.L. Xu, Q.J. Song, *ACS Appl. Mater. Interfaces* 11 (2019) 22332–22338.
- [44] T.Y. Hu, J. He, S.M. Zhang, et al., *Chem. Commun.* 54 (2018) 5760–5763.
- [45] C.F. Wang, R. Cheng, W.Q. Ji, et al., *ACS Appl. Mater. Interfaces* 10 (2018) 39205–39213.
- [46] R.K. Singh, R. Kumar, D.P. Singh, R. Savu, S.A. Moshkalev, *Mater. Today Chem.* 12 (2019) 282–314.
- [47] P. Wang, C. Liu, W.Q. Tang, et al., *ACS Appl. Mater. Interfaces* 11 (2019) 19301–19307.
- [48] S.S. Liu, C.F. Wang, C.X. Li, et al., *J. Mater. Chem. C* 2 (2014) 6477–6483.
- [49] M. Fu, F. Ehrat, Y. Wang, et al., *Nano Lett.* 15 (2015) 6030–6035.
- [50] J.Z. Shang, L. Ma, J.W. Li, et al., *Sci. Rep.* 2 (2012) 792.
- [51] S. Kalytchuk, Y. Wang, K. Polakova, R. Zboril, *ACS Appl. Mater. Interfaces* 10 (2018) 29902–29908.
- [52] B. Khalid, X.P. Bai, H.H. Wei, et al., *Nano Lett.* 17 (2017) 1140–1148.
- [53] H. Liu, S.C. Zhang, L.F. Liu, J.Y. Yu, B. Ding, *Adv. Funct. Mater.* 29 (2019) 1904108.
- [54] J.L. Wang, F. Zhang, Y.L. Wang, Y.Z. Yang, X.G. Liu, *Carbon* 126 (2018) 426–436.
- [55] H.A. Al-Attar, A.P. Monkman, *Adv. Funct. Mater.* 22 (2012) 3824–3832.
- [56] T. Yang, H. Yang, S.J. Zhen, C.Z. Huang, *ACS Appl. Mater. Interfaces* 7 (2015) 1586–1594.
- [57] S.N. Raja, A.J. Luong, W.C. Zhang, et al., *Chem. Mater.* 28 (2016) 2540–2549.